# Exchange interactions and sensitivity of the Ni two-hole spin state to Hund's coupling in doped NdNiO<sub>2</sub>

Xiangang Wan<sup>1</sup>, Vsevolod Ivanov, Giacomo Resta, Ivan Leonov<sup>1</sup>, and Sergey Y. Savrasov<sup>2</sup>

National Laboratory of Solid State Microstructures, School of Physics and Collaborative Innovation Center of Advanced Microstructures, Nanjing University, 210093 Nanjing, China

<sup>2</sup>Department of Physics and Astronomy, University of California, Davis, California 95616, USA

<sup>3</sup>M. N. Miheev Institute of Metal Physics, Russian Academy of Sciences, 620002 Yekaterinburg, Russia

<sup>4</sup>Ural Federal University, 620002 Yekaterinburg, Russia



(Received 28 August 2020; revised 12 December 2020; accepted 21 January 2021; published 11 February 2021)

Using the density-functional-based LDA+U method and linear-response theory, we study the magnetic exchange interactions of the superconductor  $Nd_{1-x}Sr_xNiO_2$ . Our calculated nearest-neighbor exchange constant  $J_1 = 82$  meV is large, weakly affected by doping, and is only slightly smaller than that found in the sister compound  $CaCuO_2$ . However, we find that the hole doping significantly enhances the interlayer exchange coupling as it affects the magnetic moment of the  $Ni-3d_{3z^2-r^2}$  orbital. This can be understood in terms of the small hybridization of  $Ni-3d_{3z^2-r^2}$  within the  $NiO_2$  plane, which results in a flat band near the Fermi level, and its large overlap along the z direction. We also demonstrate that the Nd-5d states appearing at the Fermi level do not affect the magnetic exchange interactions, and thus they may not participate in the superconductivity of this compound. Whereas many previous works emphasized the importance of the  $Ni-3d_{x^2-y^2}$  and Nd-5d orbitals, we analyze instead the solution of the  $Ni-3d_{x^2-y^2}/Ni-3d_{3z^2-r^2}$  minimal model using dynamical mean field theory. It reveals an underlying Mott insulating state that, depending on the precise values of the intra-atomic Hund's coupling smaller or larger than 0.83 eV, selects upon doping either S=0 or 1 two-hole states at low energies, leading to very different quasiparticle band structures. We propose that trends upon doping in the spin excitation spectrum and the quasiparticle density of states can be a way to probe the  $Ni 3d^8$  configuration.

### DOI: 10.1103/PhysRevB.103.075123

## I. INTRODUCTION

Since the discovery of high-temperature superconductors (HTSCs) [1], tremendous theoretical and experimental efforts have been devoted to understanding the novel physics of this family of compounds [2–4]. All HTSCs are comprised of quasi-two-dimensional  $CuO_2$  planes separated by charge reservoir spacer layers, and their parent compounds have antiferromagnetic (AFM) order with very strong inplane magnetic exchange interactions, belonging to the class of charge-transfer insulators [5]. Upon doping, holes occupy the O-2p orbital, and due to the strong hybridization between  $Cu-3d_{x^2-y^2}$  and O-2p orbitals, a Zhang-Rice singlet is formed [6]. It has been widely accepted that the HTSCs can be described by an effective single band t-J model, with different parameters explaining the variation in  $T_c$  in different materials [7,8].

Inspired by HTSCs, the search for possible novel superconducting behavior in nickelates has been attracting significant attention, as their structure and electronic configuration is similar to that of the cuprates [9–12]. Unfortunately, the monovalent Ni ion is strongly unstable and scarcely formed in mineral compounds, making, for example, LaNiO<sub>2</sub> difficult but possible to synthesize [10]. First-principles local density approximation (LDA) based calculations revealed an important difference between LaNiO<sub>2</sub> and its sister infinite-layer HTSC compound CaCuO<sub>2</sub>: the Fermi surface of CaCuO<sub>2</sub>

consists of only one two-dimensional band, while LaNiO<sub>2</sub> seems quite three-dimensional, with La-derived 5d states and Ni-3d states crossing the Fermi level [13]. Numerical calculations predicted AFM magnetic order [13,14], but magnetization and neutron powder diffraction observe no long-range order in LaNiO<sub>2</sub> [11]. At high temperatures (150 < T < 300 K), the susceptibility of LaNiO<sub>2</sub> can be fitted by the sum of a temperature-independent term and a Curie-Weiss  $S = \frac{1}{2}$  paramagnetic term with a large Weiss constant ( $\theta = -257$  K), indicating a significant correlation between Ni spins [11]. LaNiO<sub>2</sub> shows metallic behavior, but resistivity increases at lower temperatures, and no superconducting state has been observed [9–11].

Recently,  $Nd_{0.8}Sr_{0.2}NiO_2$  thin films were synthesized on a  $SrTiO_3$  substrate using soft-chemistry topotactic reduction, and superconductivity with considerably high  $T_c$  (up to 15 K) was observed [15]. The superconducting phase displays a doping-dependent dome for  $Nd_{1-x}Sr_xNiO_2$  (0.125 < x < 0.25), which is remarkably similar to that of the cuprates [16,17]. Very recently, superconductivity has also been observed in doped  $PrNiO_2$  [18].

These breakthroughs have stimulated large-scale theoretical efforts to understand the nature of the superconductivity in rare-earth nickelates. LDA band structures [19] predict that both Nd-5d and Ni-3 $d_{x^2-y^2}$  orbitals contribute significantly to the Fermi surface of parent compound NdNiO<sub>2</sub>. Most calculations treat the three 4f electrons in Nd<sup>3+</sup> as core

electrons, although the role of Nd-4f has been emphasized recently [20]. Many-body perturbative GW calculations result in almost no modification to the Fermi-surface topology and its orbital composition [21]. Focusing on the Fermi surface, different minimal models have been proposed to describe the low-energy physics of this material using a Wannier function approach, including a three-band model with Ni- $3d_{x^2-y^2}$ , Nd- $5d_{3z^2-r^2}$ , and an interstitial s orbital [22]; a three-band model with Ni- $3d_{x^2-y^2}$ , Nd- $5d_{3z^2-r^2}$ , and Nd- $5d_{3z^2-r^2}$  [25,26]; and a four-band model with Ni- $3d_{x^2-y^2}$  and Nd- $5d_{3z^2-r^2}$  [25,26]; and a four-band model [27]. The effect of topotactic hydrogen has been discussed as well [28].

Several works addressed strong correlation effects among Ni-3d electrons [29–46]. Due to a large energy difference between O-2p and Ni-3d levels, the undoped NdNiO<sub>2</sub> has been suggested to be a Mott insulator, and a coexistence/competition between low-energy S = 0 and 1 states has been proposed for the hole-doped case [29], where some Ni ions would acquire a formal  $3d^8$  configuration. The origin of these two-hole states has been discussed in recent literature [30-35]. As it is commonly accepted that the undoped Ni-3 $d^9$  configuration corresponds to the hole of  $x^2 - y^2$ symmetry, the two-hole states produced by doping can either end up as intraorbital singlets or interorbital triplets. It was first pointed out [29] that the S = 1 state may be incompatible with robust superconductivity, and indeed an exact diagonalization study of Ni impurity embedded into the oxygen environment [29] as well as a number of many-body calculations using a combination of LDA with dynamical mean field theory (DMFT) [30,33] pointed to the formation of intraorbital singlets.

The first-principles physics of competing Ni-3 $d_{x^2-y^2}$  versus Ni-3 $d_{3z^2-r^2}$ , and the connected issue of having the Ni-3 $d_{3z^2-r^2}$ states at the Fermi level with hole doping, has been first put forward in Ref. [34]. In addition, the role of Ni-3 $d_{x^2-y^2}$ and Ni- $3d_{3r^2-r^2}$  orbitals has been emphasized in Ref. [30]. A recent GW+DMFT work [36] highlighted Ni-3 $d_{3r^2-r^2}$  flatband physics as well as Ref. [37]. Furthermore, a variant of the t-J model with S = 1 has been proposed and shown to exhibit d-wave superconductivity [32]. Symmetries of the pairing states based on a two-orbital Ni-3 $d_{x^2-y^2}$ /Ni-3 $d_{xy}$ model Hamiltonian with competing S = 0 and 1 two-hole states have been discussed [31]. DMFT calculations for the two-orbital Ni-3 $d_{x^2-y^2}$ /Ni-3 $d_{3r^2-r^2}$  system argued that a multiorbital description of nickelate superconductors is necessary [35]. Excitations and superconducting instabilities have also been explored by a random phase approximation [38] and by a variant of the t-J model [39]. Local spin, charge, and orbital susceptibilities have been calculated using a combination of DMFT with a local quasiparticle self-consistent GW method, and they emphasized the Hund's physics of Ni- $e_g$ 

No sign of magnetic order has been observed in the original report on superconductivity in NdNiO<sub>2</sub> [15], which may be attributed to defects, such as unwanted hydrides or hydroxides that might form as by-products of the creation of the rare Ni<sup>+</sup> oxidation state during the synthesis of this compound. Another consideration is that LaNiO<sub>3</sub> is close to an antiferromagnetic quantum critical point (QCP) [47], therefore it is reasonable to expect that with lower dimensionality,

NdNiO<sub>2</sub> would pass the QCP and display magnetism. Very recently, strong spin fluctuations and considerable AFM exchange interactions have been observed in NdNiO<sub>2</sub> [48] as well as nuclear magnetic resonance (NMR) data [49] provided additional evidence for quasistatic AFM order below 40 K and dominant spin fluctuations at higher temperatures in Nd<sub>0.85</sub>Sr<sub>0.15</sub>NiO<sub>2</sub> bulk materials. The exchange interactions have also been discussed in several works [23,50–52]. The calculated electron-phonon interaction ( $\lambda \leq 0.32$ ) is too small to explain the 15 K  $T_c$  in this material [22], meaning the spin excitations, which are thought to be responsible for the superconductivity in HTSCs [2–4], are worth careful investigation.

In this work, based on a density functional LDA+Umethod and linear-response theory [53], we perform detailed studies of exchange interactions for both parent and doped NdNiO<sub>2</sub>. The method does not rely on a total energy analysis, and instead directly computes the exchange constant for a given wave vector  $\mathbf{q}$  based on the result of the magnetic force theorem [54]. Our results show that although the Fermi surface of undoped NdNiO2 is quite three-dimensional, its magnetic exchange interaction J has a clear two-dimensional feature with large in-plane  $J_1 = 82$  meV and much smaller out-of-plane  $J_{z1}$ . However, the Ni-3 $d_{3z^2-r^2}$  band close to the Fermi level is quite flat, therefore within the LDA+U method for a reasonable range of the values of Hubbard U above 4 eV, holes introduced by doping preferentially occupy the  $Ni-3d_{3z^2-r^2}$  orbitals while  $Ni-t_{2g}$  states remain remarkably inert. The in-plane  $J_1$  remains largely unaffected by doping, but the magnetic moment of the Ni-3 $d_{3z^2-r^2}$  orbital and the out-of-plane  $J_{71}$  both grow significantly in accord with recent findings [37]. Our calculation using a constrained-orbitalhybridization method [55] unambiguously demonstrates that while Nd-5d makes an important contribution to the Fermi surface, it has almost no effect on the magnetic exchange interaction. This result is expected, since it is known that Nd-5d orbitals have negligible hybridization with Ni orbitals [22,56]. This means that the magnetic excitations in hole-doped NdNiO2 can be described by an effective model including Ni-3 $d_{x^2-y^2}$ /Ni-3 $d_{3z^2-r^2}$  orbitals whose role has been emphasized in many recent works [19-46].

To gain additional insight, we discuss the solutions of such a two-band model on the basis of dynamical mean field theory using the parameters deduced from our band-structure calculations. In contrast to the static mean field description, such as LDA+U, where holes occupying Ni- $3d_{3z^2-r^2}$  states promote interorbital triplets, whether an S=0 or 1 state emerges from our DMFT simulation depends on a precise value of the intra-atomic Hund's coupling  $J_H$  in the vicinity of its commonly accepted range of values 0.5–1 eV. This leads to very different quasiparticle band structures. We thus propose that trends upon doping in magnetic exchange interactions and quasiparticle density of states can be a way to probe the Ni- $3d^8$  configuration.

Our paper is organized as follows. In Sec. II, we describe our  $\mathrm{LDA} + U$  and constrained-orbital-hybridization calculations for the exchange interactions. In Sec. III, we discuss a minimal two-band model that emerges from our study and its solution based on dynamical mean field theory. Section IV presents the conclusion.

#### II. CALCULATIONS OF EXCHANGE INTERACTIONS

We perform our density-functional-based electronic structure calculations within the full potential linear-muffin-tinorbital (LMTO) method [57]. To take into account the effect of on-site electron-electron interactions between Ni-3d orbitals, we add a correction due to Hubbard U using the so-called LDA+U approach [58]. Although the experimental situation of magnetism in nickelates is still unclear, hinted at by the cuprate physics, an assumption of the AFM ordered state in the parent compound should be a good starting point for a theoretical modeling. Ultimately, if AFM spin fluctuations in the doped state are responsible for superconductivity, the exchange interactions in the ordered state set the scale for those fluctuations, which justifies this assumption and provides the basis for our static linear-response calculation of J's. An alternative measure of those spin fluctuations would be a full calculation of wave vector- and frequency-dependent spin susceptibility directly in a paramagnetic state. Although possible in principle, it is a lot more involved and goes beyond the scope of this work.

We vary the parameter U for Ni-3d between 4.0 and 8.0 eV, and we find that the essential properties and our conclusions do not depend on the value of U in this range [59]. Below, we report our results for exchange constants with U = 6 eV and Hund's  $J_H = 0.95$  eV. Experimental lattice parameters have been used [15].

The magnetic exchange interactions  $J(\mathbf{q})$  were evaluated assuming a rigid rotation of atomic spins, using a previously developed linear-response approach [53]. This technique has been applied successfully to evaluate exchange interactions for a series of materials, including transition-metal oxides [53], HTSCs [60], Fe-based superconductors [61], europium monochalcogenides [62], orbitalordered noncollinear spinel MnV<sub>2</sub>O<sub>4</sub> [63], and Dirac magnon material Cu<sub>3</sub>TeO<sub>6</sub> [64]. We also use a constrained-orbitalhybridization method to provide theoretical insights into the various contributions [55] to the exchange interactions in hole doped NdNiO<sub>2</sub>. To avoid the effect of the very narrow Nd-4f bands, we shift the three occupied Nd-4f orbitals downward while shifting the rest of the Nd-4f band upward by using a constrained-orbital approach [55]. Since the obtained results do not depend on the magnitude of the shifts, we display the results with the Nd-4f bands shifted by  $\pm 2.0$  Ry.

Similarly to previously reported band-structure calculations for LaNiO<sub>2</sub> [13,22,24,27], there are two bands crossing the Fermi level in the LDA band structure of NdNiO<sub>2</sub>, with one band primarily derived from the Ni-3 $d_{x^2-y^2}$  orbital and the other consisting of predominantly Nd-5d character. Just as with LaNiO<sub>2</sub> [13,22], there is a gap between the Ni-3d and O-2p bands (around -3.5 eV). Moreover, the Ni-O bond length in NdNiO<sub>2</sub> (1.96 Å) is slightly larger than the Cu-O bond length in CaCuO<sub>2</sub> (1.92 Å). Thus the bandwidth of the Ni-3 $d_{x^2-y^2}$  band is correspondingly smaller than that of the  $Cu-3d_{x^2-y^2}$  band. While in both  $NdNiO_2$ and  $CaCuO_2$ , the  $3d_{3z^2-r^2}$  orbitals have very small dispersions along the ZRAZ line, the dispersion of the Ni-3 $d_{3z^2-r^2}$ state along  $\Gamma Z$  is considerably larger than that of Cu- $3d_{3z^2-r^2}$ . Moreover, compared to Cu- $3d_{3z^2-r^2}$ , the Ni- $3d_{3z^2-r^2}$ band lies closer to the Fermi level. These two features are expected to significantly affect the magnetic behavior in the hole doped NdNiO<sub>2</sub>.

We now perform the LDA+U calculation to examine magnetic exchange interactions in undoped NdNiO<sub>2</sub>. Our results show that the exchange coupling is large for the nearestneighbor  $J_1$  within the NiO<sub>2</sub> plane. The sign of this term is AFM, and thus the NiO<sub>2</sub> layer shows a  $(\pi, \pi)$  spin ordering. There is some debate about the magnitude of the exchange interaction, with estimates ranging from much less than that of cuprates [23,29,50] to comparable to the value of exchange interaction in CaCuO<sub>2</sub> [26,51,52]. Our calculated value of  $J_1$  is 82.24 meV as referenced to the form of the Heisenberg Hamiltonian

$$H = \frac{1}{2} \sum_{ij} J_{ij} \mathbf{S}_i \mathbf{S}_j \tag{1}$$

with S = 1/2. The estimate of  $J_1 = 25$  meV from the Raman scattering experiment of the two-magnon peak [48,50] is significantly smaller. Recent resonance x-ray scattering experiments performed for trilayer nickelate La<sub>4</sub>Ni<sub>3</sub>O<sub>8</sub> report this value to be 69 meV [65]. The in-plane  $J_1$  that we compute is only about 25% less than that found in CaCuO<sub>2</sub> [60]. We attribute it to a smaller Ni-3d and O-2p hybridization and larger energy splitting between Ni-3d and O-2p as has previously been pointed out [13]. Consistent with the result of  $(\pi, \pi, 0)$ spin ordering being slightly more energetically favorable than  $(\pi, \pi, \pi)$ , our calculation produces a small out-of-plane FM exchange interaction, with nearest neighbor  $J_{1z} = -3.4$  meV and second nearest neighbor  $J_{2z} = -23$  meV, respectively. Our calculations reveal that the magnetic moment at the Ni site (0.97 $\mu_B$ ), residing mostly in the  $3d_{x^2-y^2}$  orbital, is much larger than that at Cu sites in HSTCs.

There exists a fairly flat band right at the Fermi level along the ZRAZ line, in the band structure of the magnetic ground-state configuration of NdNiO<sub>2</sub>, as shown in Fig. 1(a). This flat band has predominantly Ni- $3d_{3z^2-r^2}$  character, and it plays an important role when hole doping is considered. The very small in-plane dispersion of the Ni- $3d_{3z^2-r^2}$  band can be understood as a consequence of the symmetry of the Ni- $3d_{3z^2-r^2}$  orbital, which can only weakly hybridize with the neighboring O-2p.

To examine the doping dependence, we perform a series of hole-doped calculations, varying the number of holes per unit cell from 0.05 to 0.30 by using the virtual crystal approximation. These calculations show that the hole doping within this range does not significantly change the shape of the band structure apart from shifting the Fermi level downward. Regardless of the hole-doping concentration, the Ni- $t_{2g}$ band is almost fully occupied and does not contribute to the magnetic moment. The magnetic moment of the Ni-3 $d_{x^2-y^2}$ orbital is also unaffected by the hole doping. Instead, the holes preferentially occupy the flat Ni- $3d_{3z^2-r^2}$  band, and, as a result, the magnetic moment of this orbital increases with doping as shown in Table I. Noting the considerable Ni-3 $d_{3z^2-r^2}$ band dispersion along  $\Gamma Z$ , and the formation of magnetic moments in this orbital, one can expect the emergence of out-of-plane magnetic exchange interactions. This result has been confirmed by our linear-response calculation. As shown in Table I, hole doping significantly enhances the out-of-plane  $J_{z1}$ , while the in-plane  $J_1$  remains mostly unaffected.

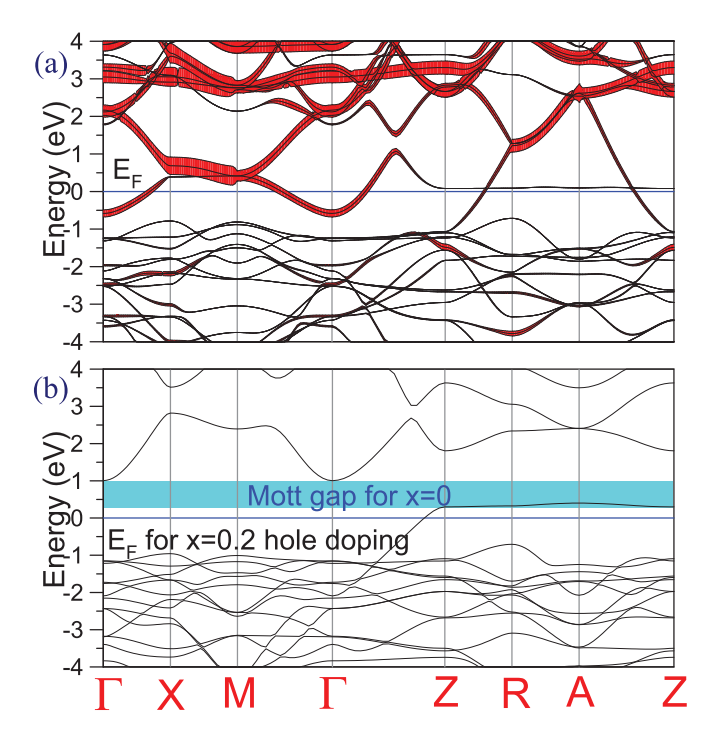


FIG. 1. Band structure of  $(\pi, \pi, 0)$  AFM ordered NdNiO<sub>2</sub> from LDA+U calculations with U=6.0 eV. (a) Undoped NdNiO<sub>2</sub> with Nd-5d orbital character shown in red; (b) constrained orbital-hybridization calculation for NdNiO<sub>2</sub> with the Nd-5d band shifted up by 2 Ry. The position of the Fermi level corresponds to 0.2 hole doping.

The 5d orbital is spatially very wide, and it can have a crucial effect on the magnetic exchange interaction through 4f-5d hybridization, even though it is empty and located above the Fermi level [62]. In NdNiO<sub>2</sub>, the Nd-5d band appears at the Fermi level, making it important to understand the role of the Nd-5d orbital in magnetic exchange interactions. We address this issue by using a constrained-orbital-hybridization approach [55]. We perform the calculations with the Nd-5d band shifted upward by various values. Figure 1(b) shows the band structure for the case in which the Nd-5d band is shifted upward by 2 Ry. As one can see, the AFM insulating state emerges from this calculation for the undoped case, while hole doping vacates the Ni- $3d_{3z^2-r^2}$  band within the  $k_z = \pi/c$  plane.

TABLE II. Calculated exchange interactions (in meV) for x = 0.2 hole doped NdNiO  $_2$ , with Nd-5d shifted upward by various energies (in Ry).

Shift (Ry)	$J_1$	$J_{z1}$
0.05	64.28	-84.04
0.10	65.48	-83.76
0.50	69.68	-75.52
2.00	71.92	-78.96

Our calculation shows that both in-plane  $J_1$  and out-ofplane  $J_{z1}$  exchange interactions are not sensitive to the position of the Nd-5d band as shown in Table II, clearly indicating that the effect of this orbital on the magnetic exchange interactions is negligible. A similar calculation was performed for LaNiO<sub>2</sub> to further confirm these findings [59]. While the obtained values of the exchange interactions are slightly different, the key features discussed above are the same.

We illustrate the effect of increasing out-of-plane exchange interactions in doped NdNiO<sub>2</sub>, using an antiferromagnetic Heisenberg model, Eq. (1). Its linear spin-wave dispersion is given by

$$\omega(\mathbf{q}) = S\sqrt{[J_{11}(\mathbf{q}) - J_{11}(0) + J_{12}(0)]^2 - [J_{12}(\mathbf{q})]^2},$$

where  $J_{11}(\mathbf{q})$  [ $J_{12}(\mathbf{q})$ ] are the exchange interactions within the same (different) sublattices. (A quantum correction factor  $Z_c \approx 1.18$ , which is sometimes used [60] in front of this formula, is omitted here.) We plot these dispersions in Fig. 2 for both undoped and 0.2 hole-doped NdNiO<sub>2</sub> in Fig. 2, along with those of CaCuO<sub>2</sub> for comparison [60]. We utilize our calculated exchange constants as a function of the wave vector for this purpose, and not their nearest-neighbor fits shown in Table I. This procedure fully accounts for the long-range effects of the interactions. Our model demonstrates some differences between the spin-wave dispersions of NdNiO2 and CaCuO<sub>2</sub>. Notably, the peak around  $(\frac{1}{2}, 0, 0)$  is reduced in NdNiO<sub>2</sub> compared with CaCuO<sub>2</sub>, as a consequence of the smaller in-plane exchange couplings, and it is largely unaffected by doping. In contrast, the out-of-plane exchange interactions strongly depend on doping, which can be seen in the changing dispersion along  $\Gamma Z$ . In undoped NdNiO<sub>2</sub>, an out-of-plane  $J_{z2}$  dominates over the vanishing nearest neighbor  $J_{z1}$ . Doping amplifies  $J_{z1}$  while suppressing  $J_{z2}$ , resulting

TABLE I. Calculated exchange interactions,  $J_1$ ,  $J_2$  (in-plane nearest, next-nearest) and  $J_{z1}$ ,  $J_{z2}$  (out-of-plane nearest, next-nearest) in meV for various hole dopings x. A positive (negative) sign denotes AFM (FM) interaction. We also list the calculated total magnetic moment at the Ni site,  $M_{\text{tot}}$ , and magnetic moment at the Ni- $3d_{3z^2-r^2}$  orbital,  $M_{3z^2-r^2}$  (in  $\mu_B$ ).

x	$J_1$	$J_2$	$J_{z1}$	$J_{z2}$	$M_{ m tot}$	$M_{3z^2-r^2}$
0.00	82.24	-4.84	-3.40	-23.00	0.97	0.17
0.05	71.84	-5.08	-21.40	-22.40	1.03	0.23
0.10	65.88	-5.68	-39.36	-18.48	1.07	0.27
0.15	64.60	-4.68	-59.04	-11.08	1.08	0.30
0.20	58.20	-4.16	-80.88	-5.56	1.15	0.35
0.25	57.36	-2.84	-97.36	-4.84	1.16	0.38
0.30	50.76	-2.16	-105.52	-2.88	1.23	0.44

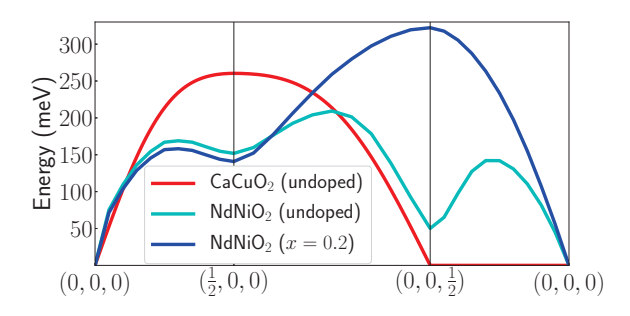


FIG. 2. Calculated spin-wave dispersions for the undoped  $NdNiO_2$  (cyan) and 0.2 hole-doped  $NdNiO_2$  (blue), with U = 6 eV. For comparison, we also plot the results of  $CaCuO_2$  (red) [60].

in the disappearance of the valley at (0, 0, 1/2) in the dispersion. Thus, in contrast with HTSCs, our calculation of J's here predicts a strongly doping-dependent resonance that could in principle be observed in neutron experiments.

#### III. TWO-BAND MODEL

A minimal model for the electronic structure of NdNiO<sub>2</sub> that emerges from the present study should involve Ni- $3d_{x^2-y^2}$  and Ni- $3d_{3z^2-r^2}$  orbitals only. Their role has already been emphasized in many recent works [19–46], and, as we argue here, their importance is based on the sensitivity of magnetic excitations to the position of various orbitals. The parameters of the model can be obtained by tracing the orbital character of these states from the nonmagnetic LDA calculation. We show this in red for Ni- $3d_{x^2-y^2}$  and in green for Ni- $3d_{3z^2-r^2}$  in Fig. 3(a). The derived two-band tight-binding model is illustrated in Fig. 3(b). In the large-U limit, such a model at a quarter filling by holes (three-electron filling) is expected

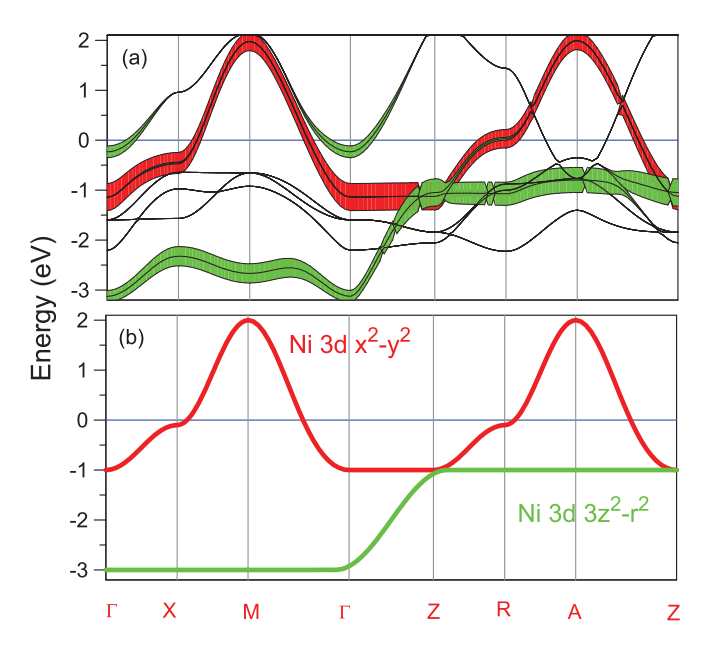


FIG. 3. (a) Nonmagnetic LDA band structure of NdNiO<sub>2</sub> with the orbital character of Ni- $3d_{x^2-y^2}$  and Ni- $3d_{3z^2-r^2}$  states shown in red and green, respectively. (b) The corresponding two-band tight-binding model [59].

to exhibit a Mott insulator for the  $3d_{x^2-y^2}$  band, with the lower Hubbard band placed below the  $3d_{3z^2-r^2}$  state. Its antiferromagnetic solution in the Hartree-Fock approximation will result in a band structure very similar to that of the LDA+U result shown in Fig. 1(b), which also assumes that the  $t_{2g}$  states of Ni, although they appear in the same energy range, are apparently irrelevant. According to our LDA+U calculation with  $U\gtrsim 4$  eV, doping sends the holes primarily to the  $3d_{3z^2-r^2}$  state promoting interorbital triplets. This is seen in Fig. 1(b), where the Fermi level shifting downward unoccupies the  $3d_{3z^2-r^2}$  band in the  $k_z=\pi/c$  plane, which explains the doping dependence of the orbital occupancies shown in Table I.

The described picture should, however, be contrasted to the genuine strong correlation effect that prompts us to consider an additional hole to be injected into either the Ni  $x^2 - y^2$  or  $3z^2 - r^2$  orbital resulting either in an intraorbital singlet or an interorbital triplet. This is different from cuprates, where holes end up in the low-lying O-2p band forming Zhang-Rice singlet states [6]. Here, it is not the relation of Hubbard U to the crystal-field splitting  $\Delta$  between  $x^2 - y^2$  and  $3z^2 - r^2$  levels but the competition of Hund's rule  $J_H$  and  $\Delta$  that should be examined to understand the origin of the two-hole state in the doped case [29,30,33–35]. To illustrate the proximity of both (S = 0 and 1) solutions, a simple diagonalization of the  $3d^8$ shell with  $U=6\,\mathrm{eV}$  and our crystal-field splitting  $\Delta=2.2\,\mathrm{eV}$ deduced from Fig. 1(b) reveals that the lowest-energy state is S = 0 for  $J_H < 0.9$  eV, and S = 1 otherwise. This value is well within the range of generally assumed Hund's rule exchange energies for transition-metal oxides and it highlights a delicate balance in extracting the two-hole ground-state configuration.

Although a number of full-fledged multiorbital LDA+DMFT calculations have been recently carried out to understand the many-body physics of doped NdNiO<sub>2</sub> [30,33,43], a strong sensitivity of the solution to the input parameters, such as  $J_H$ , is expected. This has already been highlighted in the earlier work simulating two semicircular densities of states with the crystal-field splitting as a parameter [35]. To gain additional qualitative insight, here we study our derived two-band model using dynamical mean field theory [66] and the continuous time quantum Monte Carlo method [67]. The parameters U = 6 eV and  $\Delta = 2.2$  eV are fixed while  $J_H$  is adjusted. The undoped case of the Ni- $3d^9S = 1/2$  state corresponds to the electronic filling equal to 3 in this model, where we easily recover a paramagnetic Mott insulating state with the gap of the order of U that opens up in the  $x^2 - y^2$  band and with the  $3z^2 - r^2$ states that remain completely occupied. Doping this model with 0.2 holes (filling by 2.8 electrons) results in a finite probability to find either S = 0 or 1 states in addition to S = 1/2 that depends on  $J_H$ . These probabilities extracted from the quantum Monte Carlo simulation are shown in Fig. 4 very close to our earlier estimate of 0.9 eV.

Our results for the **k**-resolved spectral functions are summarized in Fig. 5, where a comparative study is presented for the two quasiparticle band structures corresponding to the S = 0 state [ $J_H$  is set to 0.6 eV, Fig. 5(a)] and to the S = 1 state [ $J_H$  is set to 1 eV, Fig. 5(b)]. One can see from the calculated spectrum for  $J_H = 0.6$  eV that the  $3z^2 - r^2$  state remains

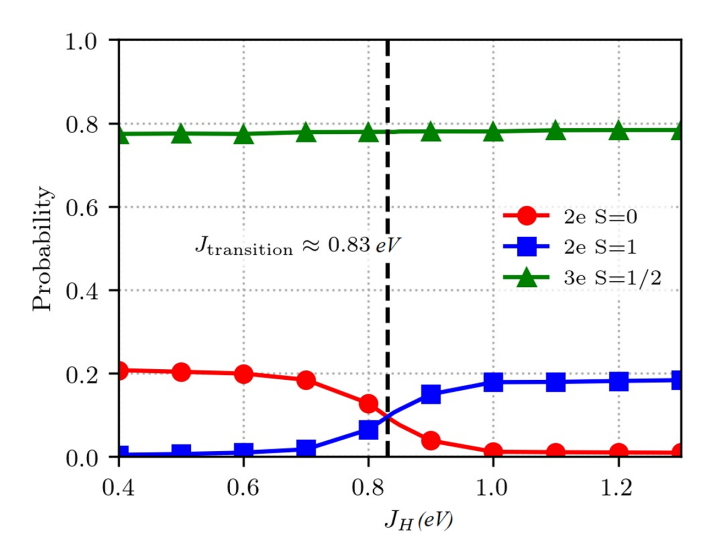


FIG. 4. Calculated probabilities for the three-electron S=1/2 and two-electron S=0 and 1 states as a function of Hund's coupling  $J_H$  using dynamical mean field theory and the continuous time quantum Monte Carlo method for the two-band model of NdNiO<sub>2</sub> corresponding to doping by 0.2 holes (filling by 2.8 electrons in the model). An inverse temperature of  $\beta=40$  is used in the calculations.

completely occupied while the doping primarily affects the  $x^2 - y^2$  band, which now shows a three-peak structure typical for DMFT with the two Hubbard bands appearing below and above the Fermi level and a renormalized quasiparticle band that crosses  $E_F$ . The k dispersion for all three features is similar to the original dispersion of the  $x^2 - y^2$  band.

A different picture emerges from the calculation with  $J_H = 1$  eV shown in Fig. 5(b). In this case, renormalized quasiparticles of  $3z^2 - r^2$  character appear at the Fermi level which illustrate the formation of the interorbital triplet states. A very strong peak in the quasiparticle density of states is expected to be present at  $E_F$  due to the nondispersive portion of the  $3z^2 - r^2$  band within the ZRA plane. At the same time, the  $x^2 - y^2$  band does not develop a three-peak structure and is characterized by the two Hubbard bands as in the undoped case. A very similar behavior was already predicted in a recent work [34], where it was termed the "Kondo resonance" property, carried by the Ni- $3z^2 - r^2$  character.

Our previous LDA+DMFT calculations [43] performed for  $J_H = 0.95$  eV are somewhat in agreement with this result, although the appearance of the flat band was detected by us earlier only at a higher doping ( $\sim$ 0.4). The origin of this discrepancy may lie in a more complex interplay between crystal fields and double counting effects in a self-consistent multiorbital simulation or in an analytical continuation of the QMC derived spectral functions resulting in a smaller and/or more broadened spectral weight as compared to the result of the model. We have additionally checked the probabilities of various spin states within LDA+DMFT, and they are mostly in line with what we observe in Fig. 4.

Since the Hund's coupling  $J_H$  of 0.8–0.9 eV is well within the range of commonly accepted values, we cannot make a definite conclusion about whether the S=0 or 1 scenario is realized for doped nickelates. However, possible future angle-resolved photoemission (ARPES) experiments may provide

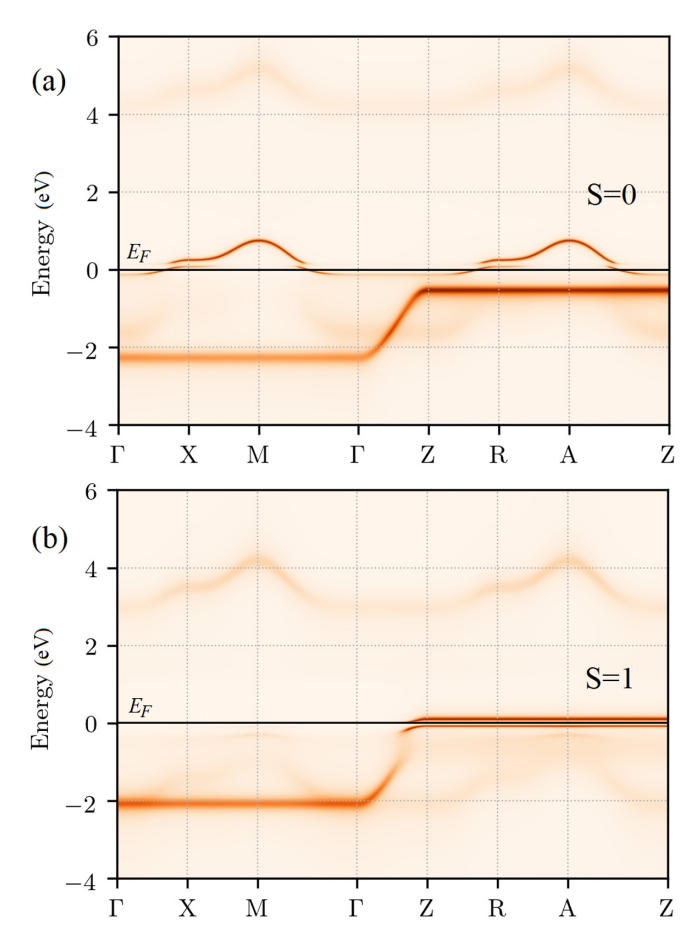


FIG. 5. Quasiparticle band structures of the two-band model of NdNiO<sub>2</sub> obtained by dynamical mean field theory and the continuous time quantum Monte Carlo method for the doping level of 0.2 holes: (a) Calculation for Hund's coupling  $J_H = 0.6$  eV that corresponds to the S = 0 two-hole state; (b) calculation for  $J_H = 1$  eV corresponding to the S = 1 two-hole state. An inverse temperature  $\beta = 40$  is used for the calculations.

important insight since, as illustrated by our calculations, the quasiparticle band structure is very different between the two cases. Furthermore, while ARPES spectra in the hole-doped HTSCs show waterfall-like behavior [68], we do not expect waterfalls to appear here due to a lack of oxygen states at energies close to  $E_F$  and associated physics responsible for the formation of the low-energy states [69].

#### IV. CONCLUSION

In conclusion, using the LDA+U method, we have calculated magnetic exchange interactions for the doped NdNiO<sub>2</sub> novel superconductor. We find that the parent compound is mostly two-dimensional, with large nearest-neighbor in-plane and small out-of-plane exchange interactions. Upon doping, the out-of-plane coupling  $J_{z1}$  was found to increase dramatically while the in-plane  $J_1$  is almost unchanged. To clarify the origin of these trends, we analyzed the symmetry of the holes induced by doping, which were found to be primarily of  $3d_{3z^2-r^2}$  character promoting the formation of an interorbital triplet as the Ni-3 $d^8$  ground-state configuration. We also investigated the role of the Nd-5d states, which

contribute substantially to the Fermi surface of NdNiO<sub>2</sub>. Shifting this band upward using a constrained-orbitalhybridization method has little effect on exchange interactions, which leads us to conclude that Nd-5d states have a negligible effect on the spin fluctuations and the superconductivity in NdNiO2. A minimal two-band model with active Ni- $3d_{x^2-y^2}$  and Ni- $3d_{3z^2-r^2}$  orbitals has been further studied with DMFT to reveal an underlying Mott insulating state, which upon doping selects either S = 0 and 1 two-hole states depending on Hund's coupling in the range of its commonly accepted values 0.8-0.9 eV. Should the S=1 state be valid, we rely on our LDA+U result to predict that upon doping, the spin susceptibility gains three-dimensionality as it gets enhanced along  $\Gamma Z$ . This can be readily observed in neutron experiments, and it can be one way to probe the two-hole configuration. We also rely on our DMFT result to predict the formation of a strong quasiparticle peak at the Fermi level detectable by ARPES experiments. A small anisotropy in  $H_{c2}$  was indeed discovered very recently [70] illustrating the three-dimensional nature of NdNiO<sub>2</sub>, which starkly contrasts with the two-dimensional superconductivity in HTSCs. At the same time, most recent x-ray absorption spectroscopy (XAS) and resonant inelastic x-ray scattering (RIXS) experiments are found to be consistent with a  $d^8$  spin singlet state [71]. These results should be important in future studies of nickelate superconductors.

#### ACKNOWLEDGMENTS

X.W. is supported by the NSFC (Grants No. 11834006, No. 11525417, No. 51721001, and No. 11790311), National Key R&D Program of China (Grants No. 2018YFA0305704 and No. 2017YFA0303203), and by 111 Project. X.W. also acknowledges the support from the Tencent Foundation through the XPLORER PRIZE. V.I., G.R., and S.Y.S. are supported by NSF DMR Grant No. 1832728. I.L. acknowledges support by the Russian Foundation for Basic Research (Project No. 18-32-20076). The DMFT electronic structure calculations were supported by the state assignment of Minobrnauki of Russia (theme "Electron" No. AAAA-A18-118020190098-5).

- [1] J. G. Bednorz and K. A. Müller, Possible high Tc superconductivity in the Ba-La-Cu-O system, Z. Phys. B 64, 189 (1986).
- [2] C. C. Tsuei and J. R. Kirtley, Pairing symmetry in cuprate superconductors, Rev. Mod. Phys. 72, 969 (2000).
- [3] D. J. Scalapino, A common thread: The pairing interaction for unconventional superconductors, Rev. Mod. Phys. 84, 1383 (2012).
- [4] P. A. Lee, N. Nagaosa, and X.-G. Wen, Doping a Mott insulator: Physics of high-temperature superconductivity, Rev. Mod. Phys. 78, 17 (2006).
- [5] J. Zaanen, G. A. Sawatzky, and J. W. Allen, Band Gaps and Electronic Structure of Transition-Metal Compounds, Phys. Rev. Lett. 55, 418 (1985).
- [6] F. C. Zhang and T. M. Rice, Effective Hamiltonian for the superconducting Cu oxides, Phys. Rev. B 37, 3759(R) (1988).
- [7] E. Pavarini, I. Dasgupta, T. Saha-Dasgupta, O. Jepsen, and O. K. Andersen, Band-Structure Trend in Hole-Doped Cuprates and Correlation with *T<sub>cmax</sub>*, Phys. Rev. Lett. **87**, 047003 (2001).
- [8] H. Sakakibara, H. Usui, K. Kuroki, R. Arita, and H. Aoki, Two-Orbital Model Explains the Higher Transition Temperature of the Single-Layer Hg-Cuprate Superconductor Compared to that of the La-Cuprate Superconductor, Phys. Rev. Lett. 105, 057003 (2010).
- [9] J. Choisnet, R. A. Evarestov, I. I. Tupitsyn, and V. A. Veryazov, Investigation of the chemical bonding in nickel mixed oxides from electronic structure calculations, J. Phys. Chem. Solids 157, 1839 (1996).
- [10] M. J. Martínez-Lope, M. T. Casais, and J. A. Alonso, Stabilization of Ni<sup>+</sup> in defect perovskites La(Ni<sub>1-x</sub>Al<sub>x</sub>)O<sub>2+x</sub> with 'infinite-layer' structure, J. Alloys Compd. **275**, 109 (1998)
- [11] M. A. Hayward, M. A. Green, M. J. Rosseinsky, and J. Sloan, Sodium hydride as a powerful reducing agent for topotactic oxide deintercalation: synthesis and characterization of the nickel(I) oxide LaNiO2, J. Am. Chem. Soc. 121, 8843 (1999).
- [12] A. Ikeda, T. Manabe, and M. Naito, Improved conductivity of infinite-layer LaNiO<sub>2</sub> thin films by metal organic decomposition, Physica C 495, 134 (2013).

- [13] K.-W. Lee and W. E. Pickett, Infinite-layer LaNiO<sub>2</sub>:  $Ni^{1+}$  is not  $Cu^{2+}$ , Phys. Rev. B **70**, 165109 (2004).
- [14] V. I. Anisimov, D. Bukhvalov, and T. M. Rice, Electronic structure of possible nickelate analogs to the cuprates, Phys. Rev. B 59, 7901 (1999).
- [15] D. Li, K. Lee, B. Y. Wang, M. Osada, S. Crossley, H. R. Lee, Yi. Cui, Y. Hikita, and H. Y. Hwang, Superconductivity in an infinite-layer nickelate, Nature (London) **572**, 624 (2019).
- [16] D. Li, B. Y. Wang, K. Lee, S. P. Harvey, M. Osada, B. H. Goodge, L. F. Kourkoutis, and H. Y. Hwang, Superconducting Dome in Nd<sub>1-x</sub>Sr<sub>x</sub>NiO<sub>2</sub> Infinite Layer Films, Phys. Rev. Lett. **125**, 027001 (2020).
- [17] S. Zeng, C. S. Tang, X. Yin, C. Li, M. Li, Z. Huang, J. Hu, W. Liu, G. Ji. Omar, H. Jani, Z. S. Lim, K. Han, D. Wan, P. Yang, S. J. Pennycook, A. T. S. Wee, and A. Ariando, Phase Diagram and Superconducting Dome of Infinite-Layer Nd<sub>1-x</sub>Sr<sub>x</sub>NiO<sub>2</sub> Thin Films, Phys. Rev. Lett. 125, 147003 (2020).
- [18] M. Osada, B. Y. Wang, B. H. Goodge, K. Lee, H. Yoon, K. Sakuma, D. Li, M. Miura, L. F. Kourkoutis, and H. Y. Hwang, A superconducting praseodymium nickelate with infinite layer structure, Nano Lett. 20, 5735 (2020).
- [19] A. S. Botana and M. R. Norman, Similarities and Differences Between LaNiO<sub>2</sub> and CaCuO<sub>2</sub> and Implications for Superconductivity, Phys. Rev. X 10, 011024 (2020).
- [20] M.-Y. Choi, K.-W. Lee, and W. E. Pickett, Role of 4f states in infinite-layer NdNiO<sub>2</sub>, Phys. Rev. B 101, 020503(R) (2020).
- [21] V. Olevano, F. Bernardini, X. Blase, and A. Cano, Ab initio many-body GW correlations in the electronic structure of LaNiO<sub>2</sub>, Phys. Rev. B **101**, 161102(R) (2020).
- [22] Y. Nomura, M. Hirayama, T. Tadano, Y. Yoshimoto, K. Nakamura, and R. Arita, Formation of a two-dimensional single-component correlated electron system and band engineering in the nickelate superconductor NdNiO<sub>2</sub>, Phys. Rev. B 100, 205138 (2019).
- [23] Z. Liu, Z. Ren, W. Zhu, Z. Wang, and J. Yang, Electronic and magnetic structure of infinite-layer NdNiO<sub>2</sub>: trace of antiferromagnetic metal, npj Quantum Mater. 5, 31 (2020).

- [24] J. Gao, S. Peng, Z. Wang, C. Fang, and H. Weng, Electronic structures and topological properties in nickelates  $Ln_{n+1}Ni_nO_{2n+2}$ , Nat. Sci. Rev., nwaa218 (2020).
- [25] M. Hepting, D. Li, C. J. Jia, H. Lu, E. Paris, Y. Tseng, X. Feng, M. Osada, E. Been, Y. Hikita, Y.-D. Chuang, Z. Hussain, K. J. Zhou, A. Nag, M. Garcia-Fernandez, M. Rossi, H. Y. Huang, D. J. Huang, Z. X. Shen, T. Schmitt, H. Y. Hwang, B. Moritz, J. Zaanen, T. P. Devereaux, and W. S. Lee, Electronic structure of the parent compound of superconducting infinite-layer nickelates, Nat. Mater. 19, 381 (2020).
- [26] E. Been, W.-S. Lee, H. Y. Hwang, Y. Cui, J. Zaanen, T. Devereaux, B. Moritz, and C. Jia, Electronic Structure Trends Across the Rare-Earth Series in Superconducting Infinite-Layer Nickelates, arXiv:2002.12300 [Phys. Rev. X (to be published)].
- [27] Y. Gu, S. Zhu, X. Wang, J. Hu, and H. Chen, A substantial hybridization between correlated Ni-d orbital and itinerant electrons in infinite-layer nickelates, Commun. Phys. **3**, 84 (2020).
- [28] L. Si, W. Xiao, J. Kaufmann, J. M. Tomczak, Y. Lu, Z. Zhong, and K. Held, Topotactic Hydrogen in Nickelate Superconductors and Akin Infinite-Layer Oxides ABO<sub>2</sub>, Phys. Rev. Lett. 124, 166402 (2020).
- [29] M. Jiang, M. Berciu, and G. A. Sawatzky, Critical Nature of the Ni Spin State in Doped NdNiO<sub>2</sub>, Phys. Rev. Lett. 124, 207004 (2020).
- [30] F. Lechermann, Late transition metal oxides with infinite-layer structure: Nickelates versus cuprates, Phys. Rev. B **101**, 081110(R) (2020).
- [31] L. H. Hu and C. Wu, Two-band model for magnetism and superconductivity in nickelates, Phys. Rev. Research 1, 032046(R) (2019).
- [32] Y.-H. Zhang and A. Vishwanath, Type–II t–J model in super-conducting nickelate  $Nd_{1-x}Sr_xNiO_2$ , Phys. Rev. Research **2**, 023112 (2020).
- [33] J. Karp, A. S. Botana, M. R. Norman, H. Park, M. Zingl, and A. Millis, Many-Body Electronic Structure of NdNiO<sub>2</sub> and CaCuO<sub>2</sub>, Phys. Rev. X **10**, 021061 (2020).
- [34] F. Lechermann, Multiorbital Processes Rule the  $Nd_{1-x}Sr_xNiO_2$  Normal State, Phys. Rev. X **10**, 041002 (2020).
- [35] P. Werner and S. Hoshino, Nickelate superconductors: Multi-orbital nature and spin freezing, Phys. Rev. B **101**, 041104(R) (2020).
- [36] F. Petocchi, V. Christiansson, F. Nilsson, F. Aryasetiawan, and P. Werner, Normal State of Nd<sub>1-x</sub>Sr<sub>x</sub>NiO<sub>2</sub> from Self-Consistent GW+EDMFT, Phys. Rev. X **10**, 041047 (2020).
- [37] M.-Y. Choi, W. E. Pickett, and K.-W. Lee, Fluctuation-frustrated flat band instabilities in NdNiO2, Phys. Rev. Res. 2, 033445 (2020).
- [38] X. Wu, D. D. Sante, T. Schwemmer, W. Hanke, H. Y. Hwang, S. Raghu, and R. Thomale, Robust  $d_{x_2-y_2}$ -wave superconductivity of infinite-layer nickelates, Phys. Rev. B **101**, 060504(R) (2020).
- [39] H. Sakakibara, H. Usui, K. Suzuki, T. Kotani, H. Aoki, and K. Kuroki, Model Construction and a Possibility of Cuprate-Like Pairing in a New d<sup>9</sup> Nickelate Superconductor (Nd, Sr)NiO<sub>2</sub>, Phys. Rev. Lett. **125**, 077003 (2020).
- [40] B. Kang, C. Melnick, P. Semon, S. Ryee, M. J. Han, G. Kotliar, and S. Choi, Infinite-layer nickelates as Ni-e<sub>g</sub> Hund's metals, arXiv:2007.14610.

- [41] Z.-J. Lang, R. Jiang, and W. Ku, Where do the doped hole carriers reside in the new superconducting nickelates? arXiv:2005.00022.
- [42] M. Kitatani, L. Si, O. Janson, R. Arita, Z. Zhong, and K. Held, Nickelate superconductors—a renaissance of the one-band Hubbard model, npj Quantum Mater. 5, 59 (2020).
- [43] I. Leonov, S. L. Skornyakov, and S. Y. Savrasov, Lifshitz transition and frustration of magnetic moments in infinite-layer NdNiO<sub>2</sub> upon hole doping, Phys. Rev. B **101**, 241108(R) (2020).
- [44] G.-M. Zhang, Y.-F. Yang, and F.-C. Zhang, Self-doped Mott insulator for parent compounds of nickelate superconductors, Phys. Rev. B **101**, 020501(R) (2020).
- [45] E. M. Nica, J. Krishna, R. Yu, Q. Si, A. S. Botana, and O. Erten, Theoretical investigation of superconductivity in trilayer square-planar nickelates, Phys. Rev. B 102, 020504(R) (2020).
- [46] T. Zhou, Y. Gao, and Z. D. Wang, Spin excitations in nickelate superconductors, Sci. China-Phys. Mech. Astron. **63**, 287412 (2020).
- [47] C. Liu, V. F. C. Humbert, T. M. Bretz-Sullivan, G. Wang, D. Hong, F. Wrobel, J. Zhang, J. D. Hoffman, J. E. Pearson, J. Samuel Jiang, C. Chang, A. Suslov, N. Mason, M. R. Norman, and A. Bhattacharya, Observation of an antiferromagnetic quantum critical point in high-purity LaNiO<sub>3</sub>, Nat. Commun. 11, 1402 (2020).
- [48] Y. Fu, L. Wang, H. Cheng, S. Pei, X. Zhou, J. Chen, S. Wang, R. Zhao, W. Jiang, C. Liu, M. Huang, X. W. Wang, Y. Zhao, D. Yu, F. Ye, S. Wang, J.-W. Mei, Core-level x-ray photoemission and Raman spectroscopy studies on electronic structures in Mott-Hubbard type nickelate oxide NdNiO<sub>2</sub>, arXiv:1911.03177.
- [49] Y. Cui, C. Li, Q. Li, X. Zhu, Z. Hu, Y.-f. Yang, J. S. Zhang, R. Yu, H.-H. Wen, and W. Yu, NMR evidence of antiferromagnetism in Nd<sub>0.85</sub>Sr<sub>0.15</sub>NiO<sub>2</sub>, arXiv:2011.09610.
- [50] H. Zhang, L. Jin, S. Wang, B. Xi, X. Shi, F. Ye, and J.-W. Mei, Effective Hamiltonian for nickelate oxides Nd<sub>1-x</sub>Sr<sub>x</sub>NiO<sub>2</sub>, Phys. Rev. Research 2, 013214 (2020).
- [51] S. Ryee, H. Yoon, T. J. Kim, M. Y. Jeong, and M. J. Han, Induced magnetic two-dimensionality by hole doping in the superconducting infinite-layer nickelate Nd<sub>1-x</sub>Sr<sub>x</sub>NiO<sub>2</sub>, Phys. Rev. B 101, 064513 (2020).
- [52] Y. Nomura, T. Nomoto, M. Hirayama, and R. Arita, Magnetic exchange coupling in cuprate-analog d<sup>9</sup> nickelates, Phys. Rev. Research **2**, 043144 (2020).
- [53] X. Wan, Q. Yin, and S. Y. Savrasov, Calculation of Magnetic Exchange Interactions in Mott-Hubbard Systems, Phys. Rev. Lett. 97, 266403 (2006).
- [54] A. I. Liechtenstein, M. I. Katsnelson, V. P. Antropov, and V. A. Gubanov, Local spin density functional approach to the theory of exchange interactions in ferromagnetic metals and alloys, J. Magn. Magn. Mater. 67, 65 (1987).
- [55] X. Wan, J. Zhou, and J. Dong, The electronic structures and magnetic properties of perovskite ruthenates from constrained orbital-hybridization calculations, Europhys. Lett. 92, 57007 (2010); Y. Du, H. Ding, L. Sheng, S. Y. Savrasov, X. Wan, and C. Duan, Microscopic origin of stereochemically active lone pair formation from orbital selective external potential calculations, J. Phys.: Condens. Matter 26, 025503 (2014).
- [56] P. Jiang, L. Si, Z. Liao, and Z. Zhong, Electronic structure of rare-earth infinite-layer RNiO<sub>2</sub> (R=La, Nd), Phys. Rev. B 100, 201106(R) (2019).

- [57] S. Y. Savrasov, Linear-response theory and lattice dynamics: A muffin-tin-orbital approach, Phys. Rev. B 54, 16470 (1996).
- [58] V. I. Anisimov, F. Aryasetiawan, and A. I. Lichtenstein, First-principles calculations of the electronic structure and spectra of strongly correlated systems: The LDA+U method, J. Phys. Condens. Matter 9, 767 (1997).
- [59] See Supplemental Material at http://link.aps.org/supplemental/ 10.1103/PhysRevB.103.075123 for additional results, supporting our conclusions.
- [60] X. Wan, T. A. Maier, and S. Y. Savrasov, Calculated magnetic exchange interactions in high-temperature superconductors, Phys. Rev. B 79, 155114 (2009).
- [61] Z. P. Yin, S. Lebegue, M. J. Han, B. P. Neal, S. Y. Savrasov, and W. E. Pickett, Electron-Hole Symmetry and Magnetic Coupling in Antiferromagnetic LaFeAsO, Phys. Rev. Lett. 101, 047001 (2008); M. J. Han, Q. Yin, W. E. Pickett, and S. Y. Savrasov, Anisotropy, Itineracy, and Magnetic Frustration in High-T<sub>C</sub> Iron Pnictides, *ibid.* 102, 107003 (2009).
- [62] X. Wan, J. Dong, and S. Y. Savrasov, Mechanism of magnetic exchange interactions in europium monochalcogenides, Phys. Rev. B 83, 205201 (2011).
- [63] R. Nanguneri and S. Y. Savrasov, Exchange constants and spin waves of the orbital-ordered noncollinear spinel MnV<sub>2</sub>O<sub>4</sub>, Phys. Rev. B 86, 085138 (2012).
- [64] D. Wang, X. Bo, F. Tang, and X. Wan, Calculated magnetic exchange interactions in the Dirac magnon material Cu<sub>3</sub>TeO<sub>6</sub>, Phys. Rev. B 99, 035160 (2019).
- [65] J. Q. Lin, P. Villar Arribi, G. Fabbris, A. S. Botana, D. Meyers, H. Miao, Y. Shen, D. G. Mazzone, J. Feng, S. G. Chiuzbaian, A. Nag, A. C. Walters, M. Garcia-Fernandez, K.-J. Zhou, J. Pelliciari, I. Jarrige, J. W. Freeland, J. Zhang, J. F. Mitchell, V. Bisogni, X. Liu, M. R. Norman, and M. P. M. Dean, Strong

- Superexchange in a  $d^{9-\delta}$  Nickelate Revealed by Resonant Inelastic X-Ray Scattering, arXiv:2008.08209 [Phys. Rev. Lett. (to be published)].
- [66] G. Kotliar, S. Y. Savrasov, K. Haule, V. S. Oudovenko, O. Parcollet, and C. A. Marianetti, Electronic structure calculations with dynamical mean-field theory, Rev. Mod. Phys. 78, 865 (2006).
- [67] K. Haule, Quantum Monte Carlo impurity solver for cluster dynamical mean-field theory and electronic structure calculations with adjustable cluster base, Phys. Rev. B 75, 155113 (2007).
- [68] F. Ronning, K. M. Shen, N. P. Armitage, A. Damascelli, D. H. Lu, Z.-X. Shen, L. L. Miller, and C. Kim, Anomalous high-energy dispersion in angle-resolved photoemission spectra from the insulating cuprate Ca<sub>2</sub>CuO<sub>2</sub>Cl<sub>2</sub>, Phys. Rev. B 71, 094518 (2005); D. S. Inosov, J. Fink, A. A. Kordyuk, S. V. Borisenko, V. B. Zabolotnyy, R. Schuster, M. Knupfer, B. Büchner, R. Follath, H. A. Dürr, W. Eberhardt, V. Hinkov, B. Keimer, and H. Berger, Momentum and Energy Dependence of the Anomalous High-Energy Dispersion in the Electronic Structure of High Temperature Superconductors, Phys. Rev. Lett. 99, 237002 (2007).
- [69] Q. Yin, A. Gordienko, X. Wan, and S. Y. Savrasov, Calculated Momentum Dependence of Zhang-Rice States in Transition Metal Oxides, Phys. Rev. Lett. 100, 066406 (2008).
- [70] Y. Xiang, Q. Li, Y. Li, H. Yang, Y. Nie, and H.-H. Wen, Magnetic transport properties of superconducting Nd<sub>1-x</sub>Sr<sub>x</sub>NiO<sub>2</sub> thin films, arXiv:2007.04884.
- [71] M. Rossi, H. Lu, A. Nag, D. Li, M. Osada, K. Lee, B. Y. Wang, S. Agrestini, M. Garcia-Fernandez, Y.-D. Chuang, Z. X. Shen, H. Y. Hwang, B. Moritz, K.-J. Zhou, T. P. Devereaux, and W. S. Lee, Orbital and spin character of doped carriers in infinite-layer nickelates, arXiv:2011.00595.